crystals

Article

β-Ga_2O_3 Used as a Saturable Sbsorber to Realize Passively Q-Switched Laser Output

Baizhong Li [1,2], Qiudi Chen [3], Peixiong Zhang [3,*], Ruifeng Tian [1,2], Lu Zhang [1,2], Qinglin Sai [1], Bin Wang [1], Mingyan Pan [1], Youchen Liu [1], Changtai Xia [1], Zhenqiang Chen [3] and Hongji Qi [1,4,*]

[1] Key Laboratory of Materials for High Power Laser, Shanghai Institute of Optics and Fine Mechanics, Chinese Academy of Sciences, Shanghai 201800, China; lbz446@siom.ac.cn (B.L.); ruifengtian@siom.ac.cn (R.T.); zhanglu@siom.ac.cn (L.Z.); saiql@siom.ac.cn (Q.S.); wangbinmars@siom.ac.cn (B.W.); pmy@siom.ac.cn (M.P.); lyc@siom.ac.cn (Y.L.); xia_ct@siom.ac.cn (C.X.)
[2] Center of Materials Science and Optoelectronics Engineering, University of Chinese Academy of Sciences, Beijing 100049, China
[3] Department of Optoelectronic Engineering, Jinan University, Guangzhou 510632, China; Cqd596918045@163.com (Q.C.); tzqchen@jnu.edu.cn (Z.C.)
[4] Hangzhou Institute of Optics and Fine Mechanics, Hangzhou 311421, China
* Correspondence: pxzhang@jnu.edu.cn (P.Z.); qhj@siom.ac.cn (H.Q.)

Abstract: β-Ga_2O_3 crystals have attracted great attention in the fields of photonics and photoelectronics because of their ultrawide band gap and high thermal conductivity. Here, a pure β-Ga_2O_3 crystal was successfully grown by the optical floating zone (OFZ) method, and was used as a saturable absorber to realize a passively Q-switched all-solid-state 1 μm laser for the first time. By placing the as-grown β-Ga_2O_3 crystal into the resonator of the Nd:GYAP solid-state laser, Q-switched pulses at the center wavelength of 1080.4 nm are generated under a output coupling of 10%. The maximum output power is 191.5 mW, while the shortest pulse width is 606.54 ns, and the maximum repetition frequency is 344.06 kHz. The maximum pulse energy and peak power are 0.567 μJ and 0.93 W, respectively. Our experimental results show that the β-Ga_2O_3 crystal has great potential in the development of an all-solid-state 1 μm pulsed laser.

Keywords: β-Ga_2O_3 crystal; optical floating zone; saturable absorber; Q-switch

check for updates

Citation: Li, B.; Chen, Q.; Zhang, P.; Tian, R.; Zhang, L.; Sai, Q.; Wang, B.; Pan, M.; Liu, Y.; Xia, C.; et al. β-Ga_2O_3 Used as a Saturable Sbsorber to Realize Passively Q-Switched Laser Output. *Crystals* **2021**, *11*, 1501. https://doi.org/10.3390/cryst11121501

Academic Editors: Xiaoming Duan, Shujun Zhang, Renqin Dou, Linjun Li and Xiaotao Yang

Received: 9 November 2021
Accepted: 29 November 2021
Published: 3 December 2021

1. Introduction

It is well known that saturable absorbers play an important role in Q-switching and mode locking operation [1–4]. Therefore, the development of different kinds of saturable absorbers as passive Q-switching devices, to achieve high-quality pulsed laser output, has always been a hot research field. At present, the research on saturable absorbers is in full swing. There are not only traditional saturable absorbers, such as dyes and transition metal ion-doped crystals, but also some new phase change materials, including bulk semiconductors and two-dimensional materials [5–9]. The pulsed laser realized by some of the materials has important application prospects in industrial processing, high-energy lasers, scientific research, and so on [10–12]. Particularly, ~1 μm near-infrared lasers, which have the advantages of high pulse energy and high peak power, can be widely used in space communication, nonlinear spectroscopy, biomedicine, military, and many other fields [13–15]. However, traditional materials often have their own shortcomings, such as limited types, single wavelength, and long-term operation stability, which need to be improved. Therefore, how to develop a stable, reliable and efficient new saturable absorber for application in the ~1 μm near-infrared band is a problem worthy of further discussion.

Ga_2O_3 is a semiconductor material with an ultra-wide band gap (~4.8 eV) and high conductivity [16,17]. Therefore, Ga_2O_3 is an electronic and optical material with great potential. Because of its unique physical and chemical properties, it has received great attention from researchers in different areas, so it has been applied in many fields, including in photo-detectors, photo-catalysis, field effect transistors, and so on [18–21]. Ga_2O_3 polymorphic, similar to Al_2O_3, which makes it particularly interesting in applications. β-Ga_2O_3 has a monoclinic structure and is the most stable phase, both physically and chemically [22,23]. β-Ga_2O_3 also inherits the excellent physical and chemical properties common to all phases of Ga_2O_3 [24,25]. These excellent properties make it clear that β-Ga_2O_3 has great potential for application in saturable absorbers. However, as far as we know, there are still no reports on the application of pure β-Ga_2O_3 crystals to saturable absorbers, and even the application of other oxide materials to saturable absorbers is rarely reported.

In terms of the β-Ga_2O_3 crystal growth method, the common large-size crystal growth method is a melting method, similarly to the Czochralski method, EFG method, Bridgman method, and so on [26–28]. We have successfully grown high-quality β-Ga_2O_3 using the optical floating zone (OFZ) method, which is a method of growing crystals without a crucible, and is usually used to study and explore the properties of materials. This method has the advantages of simple operation, few equipment requirements, and the ability to even grow crystals in the air environment. Compared with the Czochralski method, the floating zone method has the advantages of simple operation and a short cycle, and can effectively reduce the economic cost of crystal growth. Compared with the Verneuil process, the crystal quality is better [29,30]. This method solves many technical problems, such as complex equipment, difficult operation, easy introduction of impurities, inability to guarantee the growth quality, and so on. We systematically characterized the chemical and optical properties of the synthesized β-Ga_2O_3. The crystal is of good quality; it is pure and crack free. At the same time, we realized the optical modulation of β-Ga_2O_3 in pulse laser generation for the first time on the laser device with b-cut Nd:GYAP (Nd:$Gd_{0.1}Y_{0.9}AlO_3$) as the laser medium [31]. The maximum average output power is 195.1 mW, which is obtained at 1080.4 nm. The corresponding shortest pulse duration is 606.54 ns and the maximum pulse repetition rate is 344.06 kHz. The maximum single pulse energy is 0.567 μJ and the maximum peak power is 0.93 W. From the experimental results, we have obtained a relatively stable pulsed laser with a short pulse width and large repetition frequency, which shows that β-Ga_2O_3 has good saturable absorption properties. Compared with the common two-dimensional material saturable absorbers of around 1 μm, such as graphene, graphene oxide, black phosphorus (BP), topological insulators (TI), and transition metal dichalcogenides (TMDs) [5,32,33], β-Ga_2O_3, as a crystal plate, is easy to mass produce, the product performance is stable, and it is not easy to damage. The experimental results are also easy to replicate. At the same time, compared with other crystal planes used as saturable absorbers of around 1 μm, such as Cr^{4+}:YAG, Cr^{2+}:ZnS, Co^{2+}:$LaMgAl_{11}O_{19}$, and V^{3+}:YAG, the thermal conductivity of the β-Ga_2O_3 crystal is about 27 $W·m^{-1}·K^{-1}$, which is much larger than that of ZnS(0.561 $W·m^{-1}·K^{-1}$), $LaMgAl_{11}O_{19}$(2.55 $W·m^{-1}·K^{-1}$), and YAG(12.9 $W·m^{-1}·K^{-1}$) [34–40]. This indicates that the β-Ga_2O_3 crystal is favorable for the output of laser pulses with a high peak power and high repetition rate. We believe that our work will provide an important reference for the potential applications of nonlinear optical devices related to crystal growth and optical modulation.

2. The Preparation and Characterization of β-Ga_2O_3

The β-Ga_2O_3 single crystal was grown by the optical floating zone (OFZ) method, using a Quantum Design IRF01-001-00 infrared image furnace (IR Image Furnace G3, Quantum Design Japan). Ga_2O_3 powder (purity: 99.9999%, Alfa Aesar) was employed as the raw material. The raw material was pressed into a rod using a cold isostatic press. The rod was subsequently sintered at 1400 °C for 10 h in air. Moreover, a <010> oriented crystal was used as the seed. Growth was carried out using a Quantum Design IRF01-001-00 infrared image furnace. The sintered rod and seed were rotated at 10 rpm in opposite directions, and the crystal was grown in flowing air at a speed of 6 mm/h. Figure 1 shows a photo of the as-grown β-Ga_2O_3 single crystal. After growth, the as-grown sample was cut into 6 × 5 × 1 mm^3 wafers and subjected to chemical mechanical polishing to form a 0.5-millimeter-thick wafer parallel to the (100) plane to measure its optical properties.

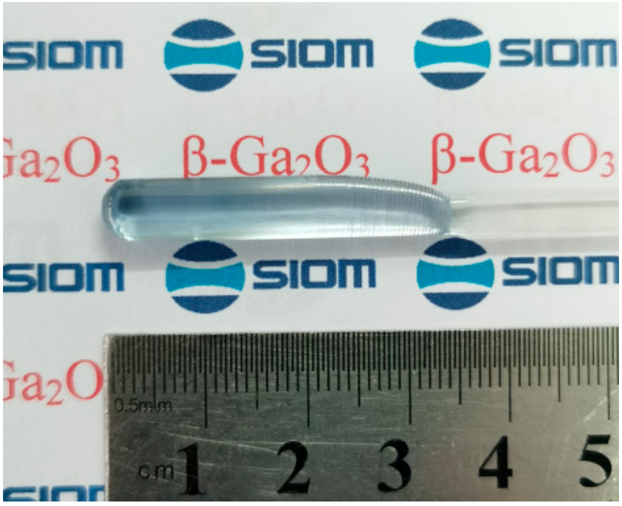

Figure 1. The photo of as-grown β-Ga_2O_3 single crystal.

The X-ray rocking curve was measured using a Bruker D8 Discover X-ray diffractometer with a Cu Kα line at 40 kV and 40 mA. The optical transmittance spectrum was collected using a Lambda 1050+ UV/Vis/NIR spectrometer (PerkinElmer). Figure 2 shows the X-ray rocking curve of the β-Ga_2O_3 (400) plane. The full width at half maximum (FWHM) is 100.8 arcsec. This shows that the β-Ga_2O_3 crystal is a single crystal with good crystallization quality. Figure 3 shows the optical transmission spectrum of the β-Ga_2O_3 single crystal. The β-Ga_2O_3 single crystal wafer indicates high transmittance, between 80% and 82%, from the visible wavelength to the infrared (IR) wavelength region. The transmittance spectrum exhibits a cutoff absorption edge at around 255 nm. This was a result of the intrinsic absorption caused by the transition from the valence band to the conduction band [41].

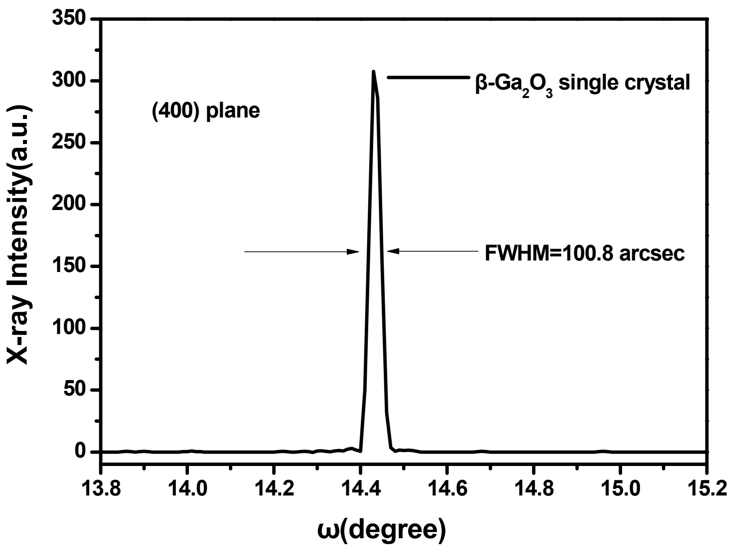

Figure 2. X-ray rocking curve of the β-Ga_2O_3 single crystal ((400) plane).

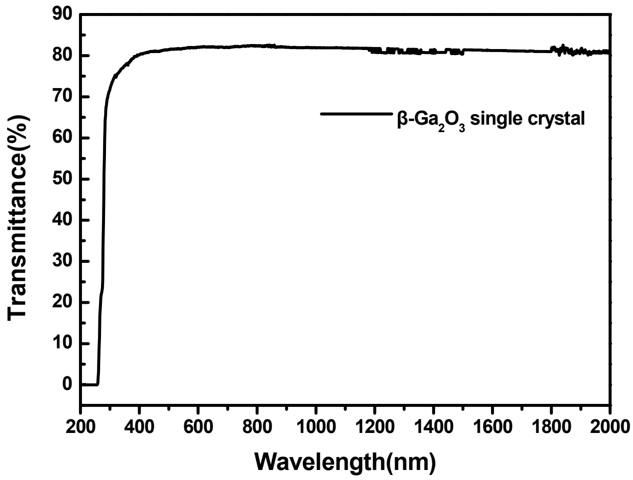

Figure 3. The optical transmission spectrum of the β-Ga_2O_3 single crystal.

3. Experimental Results and Discussion

To study the saturable absorption characteristics of β-Ga_2O_3 SA in the 1 μm wavelength region, a passively Q-switched laser, composed of a Nd:GYAP laser crystal and β-Ga_2O_3 SA, was constructed, as shown in Figure 4. The crystal was cut to a 4 × 4 × 5 mm^3 cuboid, along the b axis. The pump source is an 808 nm fiber-coupled semiconductor laser diode (LD), and the core diameter is 400 μm, with an aperture of 0.22. Using an optical imaging system (1:1 imaging module), the spot radius of the pump laser beam focused on the Nd:GYAP crystal is 200 μm. The resonator uses an input mirror M1 with high reflection from 1050 nm to 1100 nm and high transmittance from 800 nm to 820 nm, and an output mirror M2 with 10% transmittance from 1050 nm to 1100 nm. β-Ga_2O_3 SA is inserted between M2 and the gain crystal. During normal operation, the Nd:GYAP crystal is wrapped in indium foil and maintained at 17 °C by a chiller to minimize the thermal lens effect.

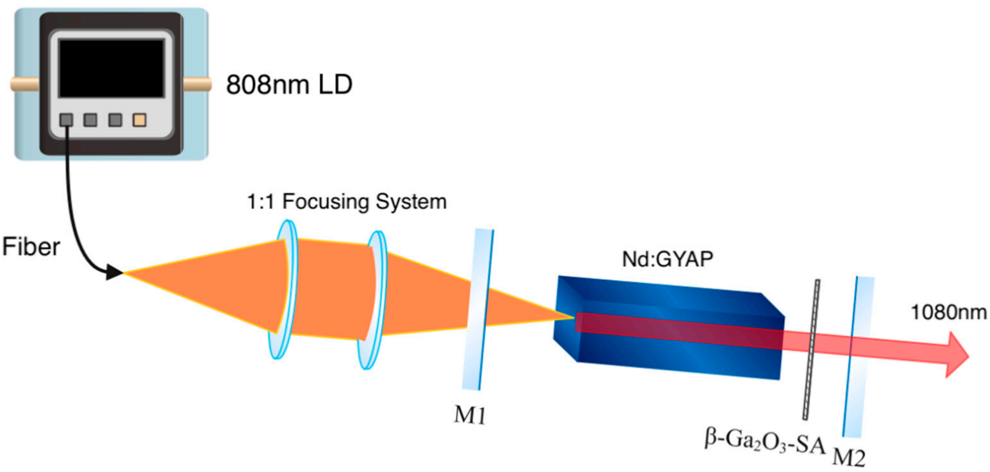

Figure 4. Schematic experimental setup of the β-Ga_2O_3 SA Q-switched Nd:GYAP laser.

When no saturable absorber is added, a continuous wave (CW), with a threshold of 0.759 W, is obtained. Then, we insert the prepared β-Ga_2O_3 SA into the laser cavity to realize the Q-switched pulse. During the experiment, the average output power of the CW and Q-switched lasers is measured as a function of pump power. It is obvious from Figure 5 that the average output power of the two groups increases linearly with the pump power. After linear fitting, the slope efficiency of the CW and Q-switched lasers are 28.6% and 10.2%, respectively. When the absorption pump power of the CW laser is 3.75 W, the maximum output power is 0.9262 W, and, at this time, it reaches the highest Q-switched average output power of 195.1 mW. The slope efficiency of the Q-switched laser is lower than that of the continuous laser, which is mainly due to the unsaturated absorption loss of Ga_2O_3 SA.

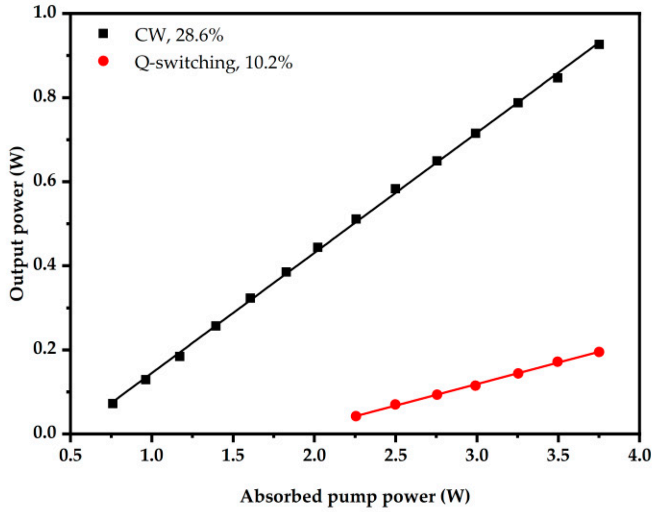

Figure 5. The average output power of Nd:GYAP laser in different operation regimes.

The pulse generation is due to the sudden decrease in the laser oscillation threshold, caused by the complete saturated absorption of SA. After the first pulse output, the absorption of SA returns to a higher initial value, and the inverted particle swarm can accumulate again to prepare for the formation of the next pulse. According to the principle of passive Q-switched pulses, at a high pump power, a short saturation absorption period and strong stimulated radiation are helpful to produce pulses with a high repetition rate and narrow pulse width, respectively. Therefore, with the increase in pump power, the duration of the Q-switched pulse narrows, and the number of pulses in the same time period increases. Figure 6 shows the variation in pulse width and repetition frequency with increasing pump power. With the increase in pump power from 2.256 W to 3.751 W, the repetition rate curve shows a continuous upward trend from 88.67 kHz to 344.06 kHz, while the width of a single pulse decreases from 2030.39 ns to 606.54 ns. Figure 7 shows the oscilloscope image at the highest repetition frequency and the shortest pulse. Through the relatively neat pulse sequence in the picture, we also know that we have obtained a relatively stable and neat pulse laser.

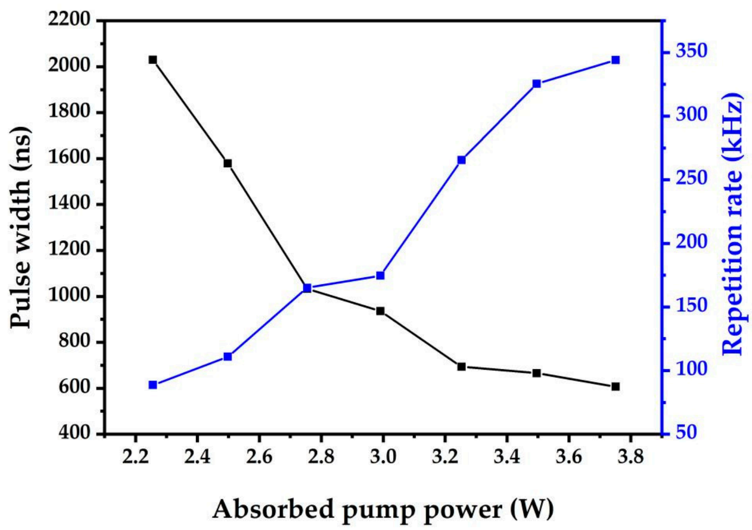

Figure 6. Dependences of pulse width and repetition rate on absorbed pump power.

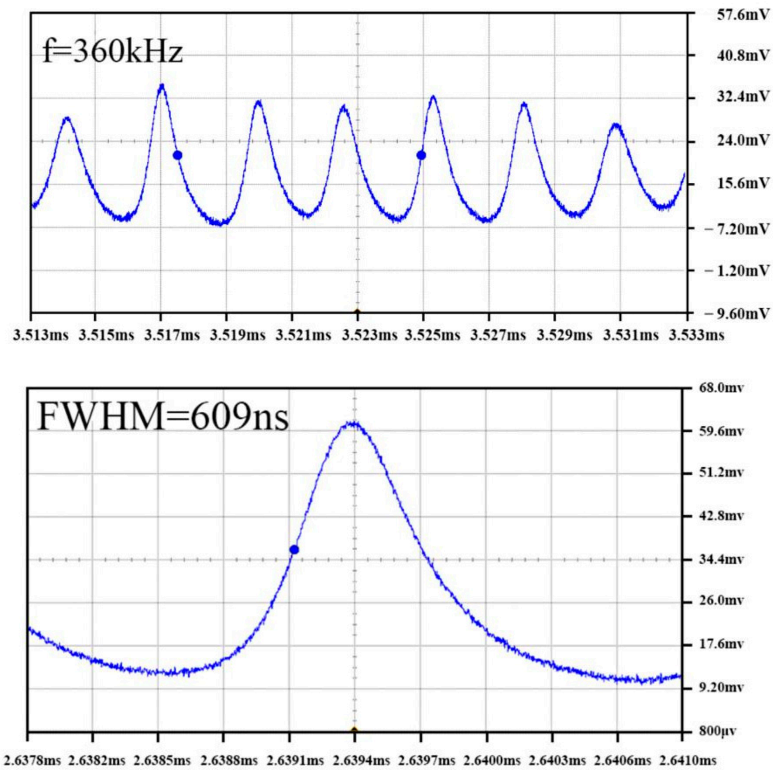

Figure 7. Temporal pulse train and single pulse profile from the β-Ga_2O_3-SA Q-switched Nd:GYAP laser.

Based on the average output power, pulse width, and repetition frequency, the corresponding single pulse energy and peak power of the Q-switched laser are calculated. The single pulse energy and peak power increase with the increase in pump power, which proves that our laser output is in Q-switched mode rather than relaxation oscillation mode. When the pump power is 3.75 W, the maximum single pulse energy is 0.567 μJ and the maximum peak power is 0.93 W. We also measured the central wavelength of laser emission. Figure 8 shows the emission wavelength in the Q-switched region, with a peak at about 1080.4 nm. The inserted β-Ga_2O_3 SA does not change the emission wavelength of the Nd:GYAP laser. Furthermore, as a stable bulk sample, as long as the laser output power and temperature do not reach the threshold of damage or crack, the β-Ga_2O_3 saturable absorber can continuously and stably output the pulsed laser and can be reused many times.

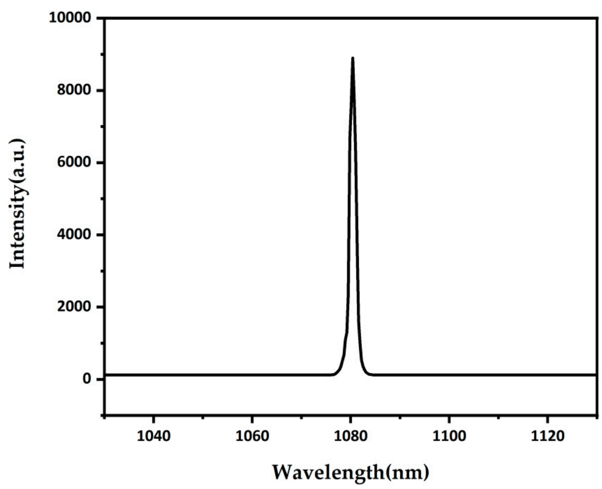

Figure 8. The laser emission spectrum of Nd:GYAP laser in Q-switching regimes.

4. Conclusions

In summary, we have successfully grown high-quality β-Ga_2O_3 used the OFZ method, and have used them as saturable absorbers, to realize the output of the pulsed laser, for the first time. The synthetic method is simple and practical, with low cost and low environmental requirements, and the grown crystal is pure and crack free. At the same time, the β-Ga_2O_3 crystal is applied to a Nd:GYAP solid-state laser for the first time, and the pulsed laser output is realized. The maximum average output power of 195.1 mW is obtained at 1080.4 nm. The corresponding minimum pulse width is 606.54 ns and the maximum pulse repetition frequency is 344.06 kHz. Our results will promote the research of more Q-switched crystals and expand their potential applications in the field of

Author Contributions: Conceptualization, B.L., P.Z. and H.Q.; data curation, B.L. and Q.C.; formal analysis, B.L., Q.C. and P.Z.; funding acquisition, P.Z., Q.S., B.W., M.P., C.X., Z.C. and H.Q.; investigation, B.L., R.T., L.Z., Q.C. and P.Z.; project administration, Y.L.; resources, Q.S., B.W., M.P. and C.X.; supervision, Z.C. and H.Q.; writing-original draft, B.L. and Q.C.; writing-review and editing, B.L., P.Z. and H.Q. All authors have read and agreed to the published version of the manuscript.

Funding: This work was supported by the National Natural Science Foundation of China (NSFC) (52072183, 52002386, 51972319, 51972149, 51872307, 61935010); the Shanghai Science and Technology Commission (20511107400); the Fundamental Research Funds for the Central Universities (21620445).

Institutional Review Board Statement: Not applicable.

Data Availability Statement: Data available in a publicly accessible repository.

Acknowledgments: In particular, we would like to thank Hangzhou Fujia Gallium Technology Co., Ltd. for its help in crystal growth and processing.

Conflicts of Interest: The authors declare no conflict of interest.

References

1. Namour, M.; Mobadder, M.; Magnin, D.; Peremans, A.; Verspecht, T.; Teughels, W.; Lamard, L.; Nammour, S.; Rompen, E. Q-Switch Nd:YAG laser-assisted decontamination of implant surface. *Dent. J.* **2019**, *7*, 99. [CrossRef]
2. Namour, M.; Verspecht, T.; Mobadder, M.; Teughels, W.; Peremans, A.; Nammour, S.; Rompen, E. Q-Switch Nd:YAG laser-assisted elimination of multi-species biofilm on titanium surfaces. *Materials* **2020**, *13*, 1573. [CrossRef] [PubMed]
3. Cong, Z.; Liu, Z.; Qin, Z.; Zhang, X.; Wang, S.; Rao, H.; Fu, Q. RTP Q-switched single-longitudinal-mode Nd:YAG laser with a twisted-mode cavity. *Appl. Opt.* **2015**, *54*, 5143–5146. [CrossRef] [PubMed]
4. Suzuki, M.; Boyraz, O.; Asghari, H.; Jalali, B. Spectral dynamics on saturable absorber in mode-locking with time stretch spectroscopy. *Sci. Rep.* **2020**, *10*, 14460. [CrossRef]
5. Ren, C.; Deng, X.; Hu, W.; Li, J.; Miao, X.; Xiao, S.; Liu, H.; Fan, Q.; Wang, K.; He, T. A near-infrared I emissive dye: Toward the application of saturable absorber and multiphoton fluorescence microscopy at the deep-tissue imaging window. *Chem. Commun. (Camb.)* **2019**, *25*, 5111–5114. [CrossRef] [PubMed]
6. Gerislioglu, B.; Bakan, G.; Ahuja, R.; Adam, J.; Mishra, Y.K.; Ahmadivand, A. The role of $Ge_2Sb_2Te_5$ in enhancing the performance of functional plasmonic devices. *Mater. Today Phys.* **2020**, *12*, 100178. [CrossRef]
7. Wang, M.; Zheng, Y.; Guo, L.; Chen, X.; Zhang, H.; Li, D. Nonlinear optical properties of zirconium diselenide and its ultra-fast modulator application. *Nanomaterials* **2019**, *9*, 1419. [CrossRef]
8. Yang, J.; Tian, K.; Li, Y.; Dou, X.; Ma, Y.; Han, W.; Xu, H.; Liu, J. Few-layer Bi_2Te_3: An effective 2D saturable absorber for passive Q-switching of compact solid-state lasers in the 1-μm region. *Opt. Express* **2018**, *26*, 21379–21389. [CrossRef]
9. Ge, W.; Zhang, H.; Wang, J.; Cheng, X.; Jiang, M.; Du, C.; Yuan, S. Pulsed laser output of LD-end-pumped 1.34 mum Nd:$GdVO_4$ laser with Co:$LaMgAl_{11}O_{19}$ crystal as saturable absorber. *Opt. Express* **2005**, *13*, 3883–3889. [CrossRef]
10. Malinauskas, M.; Žukauskas, A.; Hasegawa, S.; Hayasaki, Y.; Mizeikis, V.; Buividas, R.; Juodkazis, S. Ultrafast laser processing of materials: From science to industry. *Light Sci. Appl.* **2016**, *5*, 16133. [CrossRef]
11. Kouno, A.; Watanabe, S.; Hongo, T.; Yao, K.; Satake, K.; Okiji, T. Effect of pulse energy, pulse frequency, and tip diameter on intracanal vaporized bubble kinetics and apical pressure during laser-activated irrigation using Er:YAG Laser. *Photomed. Laser Surg.* **2020**, *38*, 431–437. [CrossRef]
12. Ge, Z.; Saito, T.; Kurose, M.; Kanda, H.; Arakawa, K.; Takeda, M. Precision interferometry for measuring wavefronts of multi-wavelength optical pickups. *Opt. Express* **2008**, *16*, 133–143. [CrossRef]
13. Griffith, R.; Simmons, B.; Bray, F.; Falto-Aizpurua, L.; Abyaneh, M.; Nouri, K. 1064 nm Q-switched Nd:YAG laser for the treatment of Argyria: A systematic review. *J. Eur. Acad. Dermatol. Venereol.* **2015**, *29*, 2100–2103. [CrossRef]

14. Chang, Y.; Lee, J.; Jhon, Y.; Lee, J. Active Q-switching in an erbium-doped fiber laser using an ultrafast silicon-based variable optical attenuator. *Opt. Express* **2011**, *19*, 26911–26916. [CrossRef] [PubMed]
15. Cabalín, L.; González, A.; Lazic, V.; Laserna, J. Deep ablation and depth profiling by laser-induced breakdown spectroscopy (LIBS) employing multi-pulse laser excitation: Application to galvanized steel. *Appl. Spectrosc.* **2011**, *65*, 797–805. [CrossRef] [PubMed]
16. Kim, S.; Lee, H.; Oh, S.; Noh, B.; Park, S.; Im, Y.; Son, S.; Song, Y.; Kim, K. Transparent conductive electrodes of β-Ga_2O_3;/Ag/β-Ga_2O_3; multilayer for ultraviolet emitters. *J. Nanosci. Nanotechnol.* **2019**, *19*, 6328–6333. [CrossRef]
17. An, Y.; Shen, X.; Hao, Y.; Guo, P.; Tang, W. Enhanced resistance switching of Ga_2O_3 thin films by ultraviolet radiation. *J. Nanosci. Nanotechnol.* **2020**, *20*, 3283–3286. [CrossRef] [PubMed]
18. Ma, J.; Yoo, G. Electrical properties of top-gate β-Ga_2O_3 nanomembrane metal-semiconductor field-effect transistor. *J. Nanosci. Nanotechnol.* **2020**, *20*, 516–519. [CrossRef]
19. Bae, H.; Yoo, T.; Yoon, Y.; Lee, I.; Kim, J.; Cho, B.; Hwang, W. High-aspect ratio β-Ga_2O_3 nanorods via hydrothermal synthesis. *Nanomaterials* **2018**, *8*, 594. [CrossRef]
20. Long, X.; Niu, W.; Wan, L.; Chen, X.; Cui, H.; Sai, Q.; Xia, C.; Devki, N.T.; Feng, Z. Optical and Electronic Energy Band Properties of Nb-Doped β-Ga_2O_3 crystals. *Crystals* **2021**, *11*, 135. [CrossRef]
21. Hisatomi, T.; Brillet, J.; Cornuz, M.; Le Formal, F.; Tétreault, N.; Sivula, K.; Grätzel, M.A. Ga_2O_3 underlayer as an isomorphic template for ultrathin hematite films toward efficient photoelectrochemical water splitting. *Faraday Discuss.* **2012**, *155*, 223–232. [CrossRef]
22. Zhou, H.; Zeng, S.; Zhang, J.; Liu, Z.; Feng, Q.; Xu, S.; Zhang, J.; Hao, Y. Comprehensive Study and Optimization of Implementing p-NiO in β-Ga_2O_3 Based Diodes via TCAD Simulation. *Crystals* **2021**, *11*, 1186. [CrossRef]
23. Reddy, L.; Ko, Y.; Yu, J. Hydrothermal synthesis and photocatalytic property of β-Ga_2O_3 nanorods. *Nanoscale Res. Lett.* **2015**, *10*, 364. [CrossRef]
24. Huan, Y.; Sun, S.; Gu, C.; Liu, W.; Ding, S.; Yu, H.; Xia, C.; Zhang, D. Recent advances in β-Ga_2O_3-Metal contacts. *Nanoscale Res. Lett.* **2018**, *13*, 246. [CrossRef]
25. Cui, W.; Ren, Q.; Zhi, Y.; Zhao, X.; Wu, Z.; Li, P.; Tang, W. Optimization of growth temperature of β-Ga_2O_3 thin films for solar-blind photodetectors. *J. Nanosci. Nanotechnol.* **2018**, *18*, 3613–3618. [CrossRef]
26. Yeom, T.; Lim, A. Study of nuclear quadrupole interactions and quadrupole Raman processes of ^{69}Ga and ^{71}Ga in a β-Ga_2O_3:Cr^{3+} single crystal. *J. Magn. Reson.* **2009**, *200*, 261–266. [CrossRef]
27. Xue, H.; He, Q.; Jian, G.; Long, S.; Pang, T.; Liu, M. An overview of the ultrawide bandgap Ga_2O_3 Semiconductor-Based schottky barrier diode for power electronics application. *Nanoscale Res. Lett.* **2018**, *13*, 290. [CrossRef]
28. Hoshikawa, K.; Kobayashi, T.; Ohba, E.; Kobayashi, T. 50mm diameter Sn-doped (001) β-Ga_2O_3 crystal growth using the Vertical Bridegman Technique in ambient air. *J. Cryst. Growth* **2020**, *546*, 125778. [CrossRef]
29. Abbene, L.; Principato, F.; Gerardi, G.; Buttacavoli, A.; Cascio, D.; Bettelli, M.; Amadè, N.; Seller, P.; Veale, M.; Fox, O.; et al. Room-temperature X-ray response of cadmium-zinc-telluride pixel detectors grown by the vertical Bridgman technique. *J. Synchrotron Radiat.* **2020**, *27*, 319–328. [CrossRef] [PubMed]
30. Kozhemyakin, G.; Nemets, L.; Bulankina, A. Simulation of ultrasound influence on melt convection for the growth of $Ga_xIn_{1-x}Sb$ and Si single crystals by the Czochralski method. *Ultrasonics* **2014**, *54*, 2165–2168. [CrossRef] [PubMed]
31. Zhou, H.; Zhu, S.; Li, Z.; Yin, H.; Zhang, P.; Chen, Z.; Fu, S.; Zhang, Q.; Lv, Q. Investigation on 1.0 and 1.3 μm laser performance of Nd^{3+}: GYAP crystal. *Opt. Laser Technol.* **2019**, *119*, 105601. [CrossRef]
32. Sun, X.; Nie, H.; He, J.; Zhao, R.; Su, X.; Wang, Y.; Zhang, B.; Wang, R.; Yang, K. Passively mode-locked 1.34 μm bulk laser based on few-layer black phosphorus saturable absorber. *Opt. Express* **2017**, *25*, 20025–20032. [CrossRef]
33. Fan, M.; Li, T.; Zhao, S.; Li, G.; Ma, H.; Gao, X.; Kränkel, C.; Huber, G. Watt-level passively Q-switched Er:Lu_2O_3 laser at 2.84 m using MoS_2. *Opt. Lett.* **2016**, *41*, 540–543. [CrossRef]
34. Zhu, H.; Chen, Y.; Lin, Y.; Gong, X.; Luo, Z.; Huang, Y. Efficient quasi-continuous-wave and passively Q-switched laser operation of a Nd^{3+}:$BaGd_2(MoO_4)_4$ cleavage plate. *Appl. Opt.* **2008**, *47*, 531–535. [CrossRef] [PubMed]
35. Yao, B.; Yuan, J.; Li, J.; Dai, T.; Duan, X.; Shen, Y.; Cui, Z.; Pan, Y. High-power Cr^{2+}:ZnS saturable absorber passively Q-switched Ho:YAG ceramic laser and its application to pumping of a mid-IR OPO. *Opt. Lett.* **2015**, *40*, 348–351. [CrossRef]
36. Li, P.; Li, Y.; Sun, Y.; Hou, X.; Zhang, H.; Wang, J. Passively Q-switched 1.34 mum Nd:$Y_xGd_{(1-x)}VO_{(4)}$ laser with Co^{2+}:$LaMgAl_{(11)}O_{(19)}$ saturable absorber. *Opt. Express* **2006**, *14*, 7730–7736. [CrossRef] [PubMed]
37. Huang, H.T.; He, J.L.; Zhang, B.T.; Yang, J.F.; Xu, J.L.; Zuo, C.H.; Tao, X.T. V^{3+}:YAG as the saturable absorber for a diode-pumped quasi-three-level dual-wavelength Nd:GGG laser. *Opt. Express* **2010**, *18*, 3352–3357. [CrossRef]
38. Kharazmi, A.; Faraji, N.; Mat Hussin, R.; Saion, E.; Yunus, W.M.; Behzad, K. Structural, optical, opto-thermal and thermal properties of ZnS-PVA nanofluids synthesized through a radiolytic approach. *Beilstein J. Nanotechnol.* **2015**, *6*, 529–536. [CrossRef]
39. Guo, Z.; Verma, A.; Wu, X.F.; Sun, F.Y.; Hickman, A.; Masui, T.; Kuramata, A.; Higashiwaki, M.; Jena, D.; Luo, T.F. Anisotropic thermal conductivity in single crystal β-gallium oxide. *Appl. Phys. Lett.* **2015**, *106*, 1–5. [CrossRef]
40. Sun, J.B.; Niu, L.F.; Hui, Y.L.; Chen, W.Y.; Wang, X.L.; Lu, J.S.; Wei, H. Thermal conductivity and compatibility of $LaMgAl_{11}O_{19}/LaPO_4$ composites. *Ceram. Int.* **2020**, *46*, 27967–27972. [CrossRef]
41. Li, P.; Bu, Y.; Chen, D.; Sai, Q.; Qi, H. Investigation of the crack extending downward along the seed of the β-Ga_2O_3 crystal grown by the EFG method. *CrystEngComm* **2021**, *23*, 6300–6306. [CrossRef]